

Ab Initio Calculations of p -Shell Nuclei with JISP16

Pieter Maris

Department of Physics and Astronomy, Iowa State University, Ames, IA 50011, USA

Abstract

I present an overview of binding energies and ground state magnetic moments for p -shell nuclei calculated with the phenomenological NN interaction JISP16, and compare with experimental data. I also illustrate how the decomposition of total angular momentum into intrinsic spin and orbital components can provide insights into the structure of states and relationships among states.

Keywords: *Nuclear structure; ab initio; configuration interaction; JISP16*

1 No-Core Full Configuration approach

In the Configuration Interaction (CI) approach to describe quantum many-body systems, the many-body Schrödinger equation

$$H \Psi_i(\mathbf{r}_1, \dots, \mathbf{r}_A) = E_i \Psi_i(\mathbf{r}_1, \dots, \mathbf{r}_A) \quad (1)$$

becomes a large sparse matrix problem with eigenvalues E_i and eigenvectors Ψ_i representing the A -body wavefunctions. For No-Core nuclear structure calculations [1] the wavefunction Ψ of a nucleus consisting of A nucleons is expanded in an A -body basis of Slater determinants Φ_k of single-particle wavefunctions $\phi_{nljm}(\mathbf{r})$,

$$\Psi(\mathbf{r}_1, \dots, \mathbf{r}_A) = \sum c_k \Phi_k(\mathbf{r}_1, \dots, \mathbf{r}_A), \quad (2)$$

with $\Phi_k(\mathbf{r}_1, \dots, \mathbf{r}_A) = \mathcal{A}[\phi_{n_1 l_1 j_1 m_1}(\mathbf{r}_1) \phi_{n_2 l_2 j_2 m_2}(\mathbf{r}_2) \dots \phi_{n_A l_A j_A m_A}(\mathbf{r}_A)]$ and \mathcal{A} is the antisymmetrization operation. Conventionally, one uses a harmonic oscillator (HO) basis for the single-particle wavefunctions, which are labelled by their quantum numbers n , l , j , and m ; n and l are the radial and orbital HO quantum numbers (with $N = 2n + l$ the number of HO quanta), j is the total single-particle spin, and m its projection along the z -axis. The many-body basis states Φ_k have well-defined parity, $(-1)^{\sum_A l_i}$, and total spin-projection, $M = \sum_A m_i$, but they do not have a well-defined total spin J . Thus, in two runs (one for each parity), one can obtain the complete low-lying spectrum, including the ground state, even if the spin of the ground state is not known a priori.

The many-body Hamiltonian H in Eq. (1) can be expressed in terms of the relative kinetic energy plus 2-body, 3-body, and, in general, up to A -body interaction terms

$$H = T_{\text{rel}} + V_{\text{Coulomb}} + V_{NN} + V_{N\bar{N}N} + \dots \quad (3)$$

Here I focus on results obtained with the phenomenological 2-body (NN) interaction JISP16. This interaction is constructed from inverse scattering analysis of the neutron-proton phase shifts; subsequently its off-shell behavior is tuned to reproduce the deuteron properties as well as select additional light nuclear properties using

Proceedings of International Conference ‘Nuclear Theory in the Supercomputing Era — 2013’ (NTSE-2013), Ames, IA, USA, May 13–17, 2013. Eds. A. M. Shirokov and A. I. Mazur. Pacific National University, Khabarovsk, Russia, 2014, p. 37.
<http://www.ntse-2013.khb.ru/Proc/Maris.pdf>.

phase-shift equivalent unitary transformations [2]. The resulting NN interaction is charge-independent; the only charge dependence comes from the Coulomb interaction V_{Coulomb} in Eq. (3).

A convenient and efficient truncation of the complete (infinite-dimensional) basis is a truncation on the total number of HO quanta of the many-body basis: the basis is limited to many-body basis states with $\sum_A N_i \leq N_0 + N_{\text{max}}$. Here, N_i is the number of quanta of each single-particle state; N_0 is the minimal number of quanta for that nucleus; and N_{max} is the truncation parameter. Note that for HO single-particle states, this truncation leads to an exact factorization of the center-of-mass wavefunction and the relative wavefunction [3].

Any CI calculation, using a finite truncation of the complete basis, gives a strict upperbound for the lowest states of each spin and parity for a given nuclear potential. In the No-Core Full Configuration (NCFC) approach [4] one is interested in the convergence with increasing basis space dimensions and thus recover, to within quantifiable uncertainties, results corresponding to the complete basis. In order to do so, one has to address eigenvalue problems for increasingly large matrices, with dimensions of well over a billion. Improved algorithms to construct these matrices and to determine their lowest eigenstates, as well as efficient use of increasing computational resources are critical for the success of this approach [5–10].

The empirical model used for the extrapolation of the (ground state) energies to the complete basis is [4]

$$E(\hbar\omega, N_{\text{max}}) = E_{\infty} + a_{\hbar\omega} e^{-b_{\hbar\omega} N_{\text{max}}}, \quad (4)$$

where $\hbar\omega$ is the HO energy. I use sets of three consecutive N_{max} values at fixed values of $\hbar\omega$ to estimate the energy in the complete basis. Extrapolations based on calculations up to N_{max} are using results from the $(N_{\text{max}} - 4)$, $(N_{\text{max}} - 2)$, and N_{max} bases for the extrapolation, and the difference with the extrapolation of the $(N_{\text{max}} - 6)$, $(N_{\text{max}} - 4)$, and $(N_{\text{max}} - 2)$ bases is used as an estimate of the extrapolation uncertainty. For this extrapolation method one needs results up to at least $N_{\text{max}} = 8$.

For consistency, I then check that (1) extrapolations at different $\hbar\omega$ values are within each other's uncertainty estimates; (2) as N_{max} increases, the extrapolations are within the uncertainty estimates of smaller N_{max} values; and (3) numerical uncertainty estimates decrease as N_{max} increases. This is all done at fixed $\hbar\omega$; the final result for E_{∞} is the extrapolated result at that $\hbar\omega$ value for which the amount of extrapolation is minimal, i. e. the point where $E(\hbar\omega, N_{\text{max}}) - E_{\infty}$ is minimal. Typically, with JISP16, this is at or slightly above the $\hbar\omega$ value that minimizes the (ground-state) energy in finite bases. The final error estimate is enlarged as necessary in order to get consistent results, such that the central values are within the final numerical error estimate over a 10 MeV range around the variational minimum. (Note that in the original version of this extrapolation [4] we did not make such an adjustment.)

2 Ground state energies with JISP16

This extrapolation method is illustrated in the left panel of Fig. 1 for the ground state of ${}^7\text{Li}$. As one can see in this figure, the error estimates are minimal around the variational minimum in $\hbar\omega$; furthermore, extrapolations based on the three data points at the largest N_{max} do indeed fall within the error estimates of the previous extrapolations, and do have smaller error estimates. However, there seems to be a systematic $\hbar\omega$ dependence of the extrapolated results suggesting that Eq. (4) is not the correct asymptotic behavior. Indeed, recent studies [11–14] of the effective infrared and ultraviolet cutoffs of a finite HO basis have shown that the asymptotic behavior contains a term that is exponential in $\sqrt{N_{\text{max}}}$, in addition to a term that is exponential in N_{max} . The uncertainty analysis of these extrapolation methods is still under

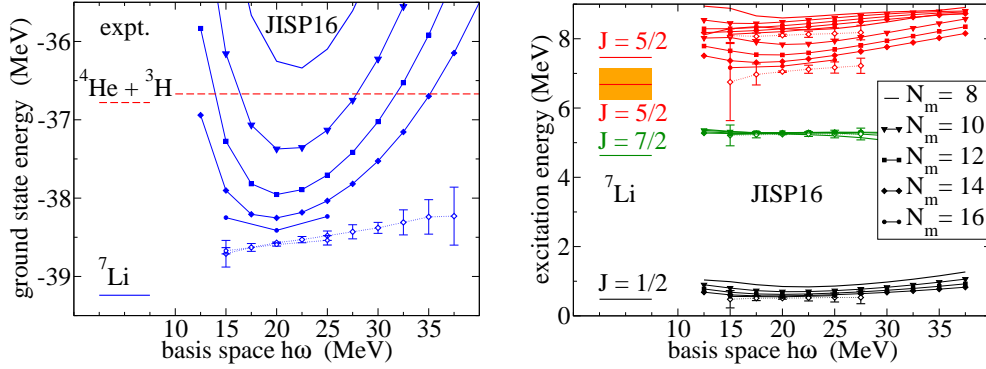


Figure 1: Ground state energy (left) and low-lying spectrum for ${}^7\text{Li}$ (right). Extrapolated energies are depicted with open symbols connected by dotted lines.

investigation; once their uncertainties have been quantified, these extrapolations are likely to become more valuable.

In Fig. 2 I present a summary of ground state energies of light nuclei up to ${}^{16}\text{O}$ calculated with JISP16 in the NCFC approach [15]. For $A = 3$ and $A = 4$, as well as for ${}^6\text{He}$ and ${}^6\text{Li}$, our results are in excellent agreement with calculations using the hyperspherical harmonics approach [16, 17]. In recent years, JISP16 has been used successfully to benchmark novel truncation methods for *ab initio* CI calculations, such as the No-Core Monte Carlo Shell Model [18, 19] and the Symmetry-Adapted No-Core Shell Model [20, 21], as well calculations based on Coulomb–Sturmian single-particle wavefunctions [22] and calculations in a Wood–Saxon basis [23] — each of these methods yields results consistent with the results presented here.

There is a reasonable overall agreement between the calculated and experimental binding energies: for $A = 6$ to 10 JISP16 underbinds slightly, but starting from $A = 12$, JISP16 overbinds the $T = 0$ and $T = \frac{1}{2}$ states by an amount that increases with A , but decreases with T . This trend towards overbinding of the $N = Z$

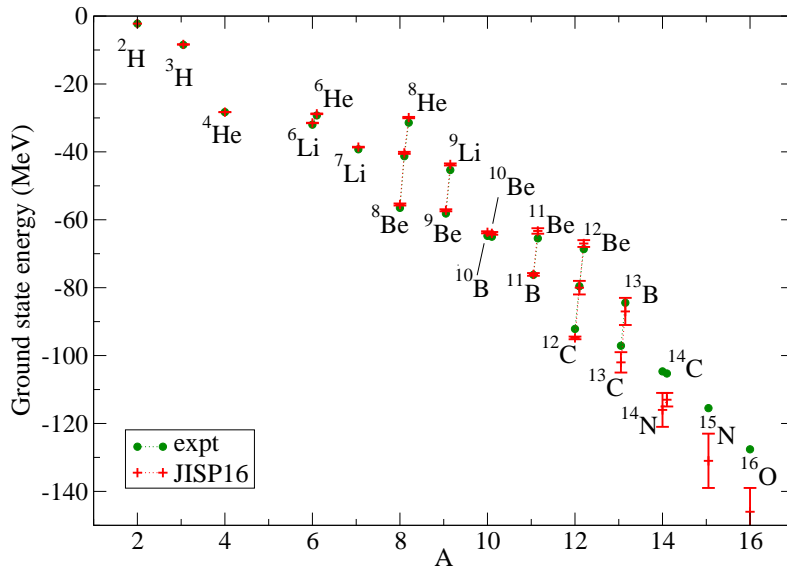


Figure 2: Ground state energy for $A = 2$ to $A = 16$ with JISP16, including numerical uncertainty estimates (only one ground state for each A and T), compared to experimental data.

nuclei starting from ^{12}C has been noted earlier [4], and can be remedied by a further tuning of the off-shell behavior of the NN interaction [24].

3 Excited states

Most known excited states in p -shell nuclei are particle (or cluster) unstable but many have widths less than a few hundred keV. For such narrow states the real part of the S -matrix poles may be well-approximated by the eigenenergies calculated in a HO basis [25]. E. g., for ^7Li the first excited state, with $J^\pi = \frac{1}{2}^-$, is below the threshold for ^4He plus ^3H , but the next excited states state, at about 5 MeV with $J^\pi = \frac{7}{2}^-$, is well above this threshold. Nevertheless, the excitation energy of this state is very well converged, see the right panel of Fig. 1, and one does not really need any extrapolation for the excitation energies of these two lowest excited states [26].

The excitation energies of the two $J^\pi = \frac{5}{2}^-$ states around 7 to 8 MeV however are not as well converged, and do depend on the basis parameters. Even after the exponential extrapolation to a complete basis, the excitation energies shows a systematic dependence on the basis parameter $\hbar\omega$, in particular for the first $J^\pi = \frac{5}{2}^-$ state. This behavior is characteristic for resonances in a pure HO basis, and one might get better converged results using an approach that incorporates continuum states [27–29]. Nevertheless, one can conclude that with JISP16 the excitation energies for the lowest four excited states in ^7Li are all within about 10% to 15% of the experimental values.

Experimentally, the lowest $J^\pi = \frac{5}{2}^-$ state is broad, whereas the second $J^\pi = \frac{5}{2}^-$ is narrow; not much else is known to distinguish them. Our calculations [26] however indicate that these two states have a very different structure: the first $J^\pi = \frac{5}{2}^-$ has a large negative quadrupole moment, whereas the second has a moderately large positive quadrupole moment. Furthermore, the first $J^\pi = \frac{5}{2}^-$ state has a moderately strong $B(E2)$ transition to the $J^\pi = \frac{3}{2}^-$ ground state, whereas the $B(E2)$ transition from the second $J^\pi = \frac{5}{2}^-$ state is more than an order of magnitude smaller.

In order to get a better understanding of the structure of these (and other) states, one can also look at their spin structure. The contributions to the total spin \mathbf{J} in terms of the nucleon intrinsic spin, \mathbf{S} , and orbital motion, \mathbf{L} , is given by

$$J = \frac{1}{J+1} \left(\langle \mathbf{J} \cdot \mathbf{L}_p \rangle + \langle \mathbf{J} \cdot \mathbf{L}_n \rangle + \langle \mathbf{J} \cdot \mathbf{S}_p \rangle + \langle \mathbf{J} \cdot \mathbf{S}_n \rangle \right). \quad (5)$$

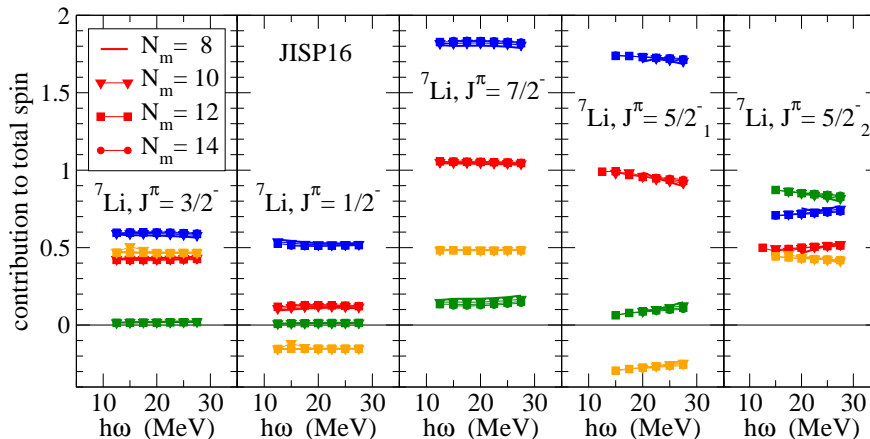


Figure 3: Contribution to the total spin of select states of ^7Li from the proton orbital motion (red), neutron orbital motion (blue), proton intrinsic spin (orange), and neutron intrinsic spin (green). Adapted from Ref. [15].

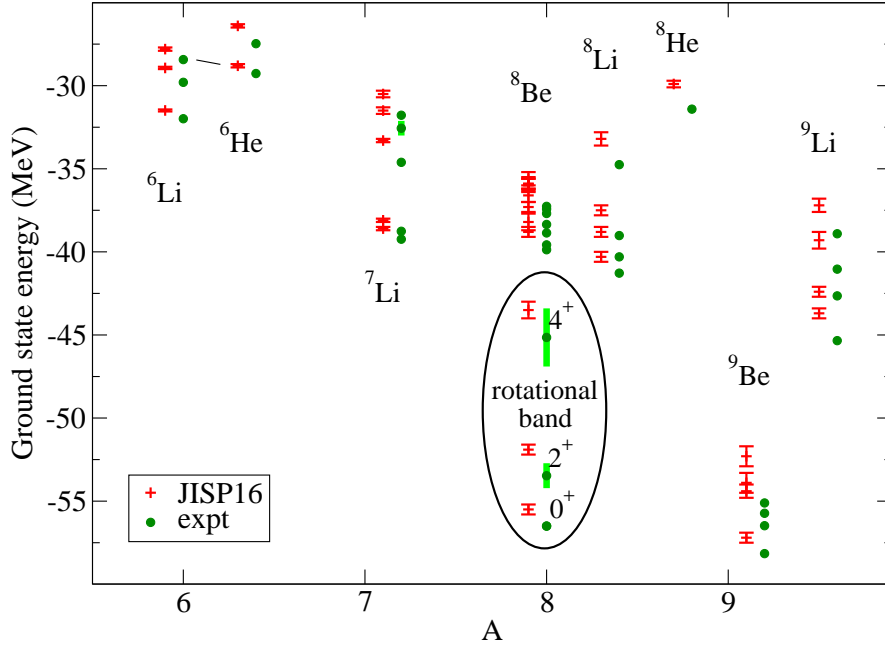


Figure 4: Energies of select low-lying states for $A = 6$ to $A = 9$ with JISP16, including numerical uncertainty estimates, compared to experimental data.

Generally (though not always) these components converge rather quickly. In Fig. 3 these components are shown for the five lowest states in ${}^7\text{Li}$. Clearly, the first and second $\frac{5}{2}^-$ and $\frac{5}{2}^-$ states have a very different structure, despite being very close in energy: they differ significantly in all their spin components. A closer look at both the quadrupole moments and the spin components of the lowest four states suggests that these states (with $J^\pi = \frac{1}{2}^-, \frac{3}{2}^-, \frac{5}{2}_1^-, \text{ and } \frac{7}{2}^-$) form a rotational band. Also the $B(E2)$ and $B(M1)$ transition strengths between these states are in qualitative agreement with predictions based on a rotational structure [30].

In Fig. 4 I summarize results for both the ground states and select excited states for $A = 6$ to $A = 9$, after extrapolation to the complete basis. As already noted, JISP16 slightly underbinds these nuclei, but the excitation energies are generally in qualitative agreement with the data, as can be seen in Fig. 4: for most of these nuclei the calculated results (red plusses) seem all to be shifted upwards by a constant (nucleus-dependent) amount, reproducing the experimental spectrum quite well. Also the calculated spin and parity of the states shown in Fig. 4 agrees with the experimentally assigned spin-parity.

4 Beryllium isotopes

It is known that the low-lying states in both ${}^8\text{Be}$ and ${}^9\text{Be}$ are members of rotational bands. Indeed, the excitation energies of the first 2^+ and 4^+ states of ${}^8\text{Be}$, see Fig. 4, follow the rotational pattern. Although the quadrupole moments themselves are not (yet) converged, the ratio of the quadrupole moments of the first 2^+ and 4^+ states of ${}^8\text{Be}$ are in good agreement with a rotational model, as are their $B(E2)$ transition strength (relative to the intrinsic quadrupole moment) [30].

Starting with ${}^8\text{Be}$, narrow states of both parities appear in the experimental spectrum; and for ${}^{11}\text{Be}$ the lowest positive parity state is the ground state, contrary to the expectations based on the shell model, which predicts negative parity ground states for all odd *p*-shell nuclei. For ${}^7\text{Be}$ through ${}^{13}\text{Be}$ I performed calculations for

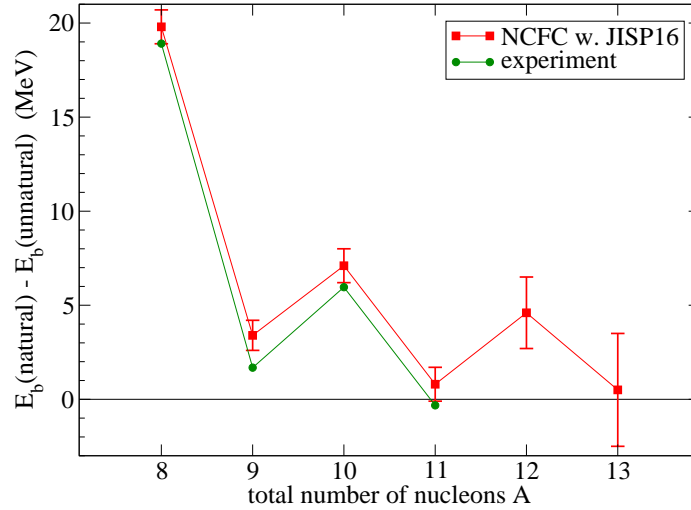


Figure 5: Energy difference between lowest positive and negative parity states for Beryllium isotopes. Adapted from Ref. [31].

both natural and unnatural parity states. Figure 5 shows the difference between the extrapolated binding energy of the lowest natural parity state and the lowest unnatural parity state [31], treating the extrapolation uncertainties as independent. One expects this difference to be positive, but for isotopes with parity inversion it becomes negative. Although JISP16 does not quite reproduce the observed parity inversion for ^{11}Be , parity inversion is within the numerical error estimates for this isotope. Furthermore, over the range of isotopes from ^8Be to ^{11}Be the results are in very good qualitative agreement with the data: JISP16 seems to underbind all unnatural parity states by a similar amount of about 1 MeV. Based on these results, I also predict parity inversion for ^{13}Be ; experimentally, the parity of the ground state is not confirmed, though likely to be negative [32], which indeed implies parity inversion (^{13}Be has one neutron in the sd -shell, so the natural parity is positive).

The negative parity spectrum and positive parity spectrum of ^9Be , relative to the lowest state of that parity, is shown in Fig. 6. The excitation energies of the lowest $\frac{5}{2}^-$ and $\frac{7}{2}^-$ states are quite well converged, in contrast to excitation energies of the $\frac{1}{2}^-$, the $\frac{3}{2}^-$, and the second $\frac{5}{2}^-$ states. This difference in convergence rate can be understood by the observation that the ground state forms a rotational band with

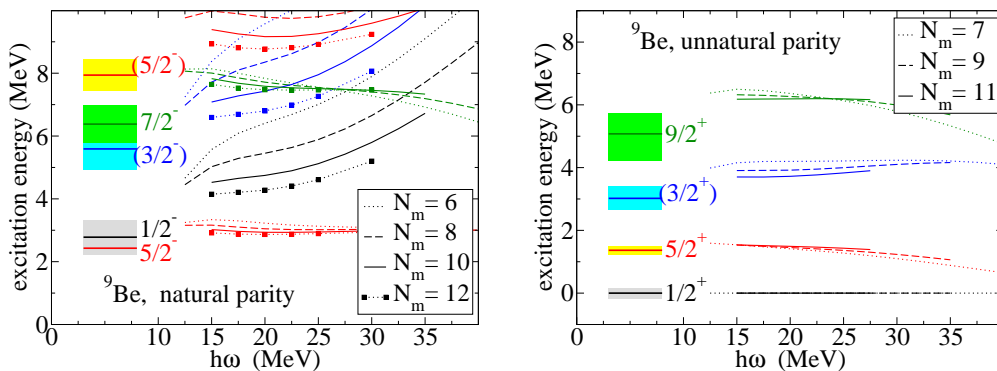


Figure 6: Excitation energies of the lowest excited states of ^9Be with negative parity (left) and positive parity (right), relative to the lowest state of that parity.

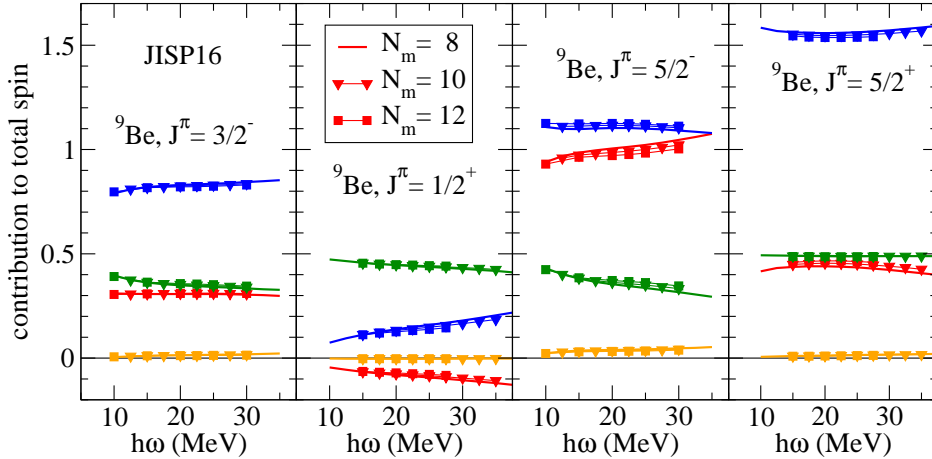


Figure 7: Contribution to the total spin of select states of ${}^9\text{Be}$ from the proton orbital motion (red), neutron orbital motion (blue), proton intrinsic spin (orange), and neutron intrinsic spin (green). Adapted from Ref. [15].

the lowest $\frac{5}{2}^-$ and $\frac{7}{2}^-$ states, and the corresponding wavefunctions have therefore a similar structure, and are likely to converge at a similar rate. The low-lying positive parity states also form a rotational band, and indeed, their excitation energies, relative to the $\frac{1}{2}^+$ state, are also quite well converged at $N_{\text{max}} = 11$. Note however that the excitation energy of the positive parity states relative to the (negative parity) ground state are not as well converged, and can only be calculated after extrapolation to the complete basis [15].

In Fig. 7 I show the spin contributions for the lowest two negative parity states and for the lowest two positive parity states of ${}^9\text{Be}$. In all four states, the contribution from the neutron intrinsic spin is close to $\frac{1}{2}$, and that from the proton intrinsic spin is nearly zero. This is consistent with a cluster configuration of two α -particles and a neutron for these states. The observed spin contributions for the ground state $J^\pi = \frac{3}{2}^-$ suggests that this state is dominated by an α -cluster configuration of two α -particles plus a neutron in a π -orbital, in which the neutron orbital motion contributes one unit to the total angular momentum. The ground state proton and neutron density distributions are consistent with this interpretation as well [31]. On the other hand, the lowest positive parity state, $J^\pi = \frac{1}{2}^+$, is likely to be dominated by two α -particles plus a neutron in a σ -orbital. The $\frac{5}{2}^-$ and $\frac{5}{2}^+$ states can then be interpreted as rotational excitations of these two states, with most of the total angular momentum coming from orbital motion of the nucleons. Indeed, calculations of the quadrupole moments and $B(E2)$ transition strengths of these states are also in agreement with these states forming rotational bands [30].

5 Magnetic moments

Using the canonical 1-body current operator, the magnetic moments in impulse approximation follow from the spin components

$$\mu = \frac{1}{J+1} \left(\langle \mathbf{J} \cdot \mathbf{L}_p \rangle + 5.586 \langle \mathbf{J} \cdot \mathbf{S}_p \rangle - 3.826 \langle \mathbf{J} \cdot \mathbf{S}_n \rangle \right) \mu_0. \quad (6)$$

In Fig. 8 I show results for the magnetic moments of the ground states of p -shell nuclei. Typically, the calculated results are within about 0.3μ of the experimental

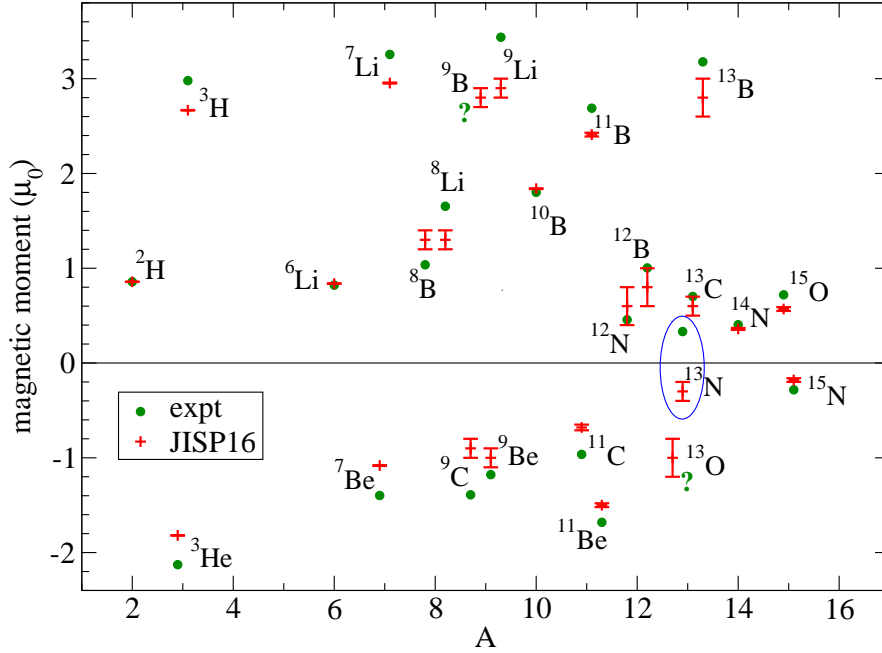


Figure 8: Ground state magnetic moments for $A = 2$ to $A = 16$ with JISP16, including numerical uncertainty estimates, compared to experimental data.

data. This discrepancy is likely due to the omission of 2-body currents; with consistent 2-body currents, one expects to get much better agreement with the data. However, since JISP16 is a purely phenomenological potential, it is not clear how to construct a consistent 2-body current, whereas for a microscopic interaction such as chiral interactions or a phenomenological meson-exchange potential like AV18, one can use consistent meson-exchange currents, and find generally good agreement with the data once meson-exchange currents are included [33,34].

Some of the largest deviations between the impulse approximation calculations and the experimental data are for the ground states of ${}^9\text{Li}$ and ${}^9\text{C}$. It is interesting to note that also with AV18 plus IL7 3-body force there is a similarly large discrepancy between impulse approximation calculations and data for these two states. For the AV18 plus IL7 it has been shown that meson-exchange currents contribute $+0.70(2)\mu$ and $-0.60(3)\mu$ respectively to these magnetic moments, and with these corrections included, the results for ${}^9\text{Li}$ and ${}^9\text{C}$ are in agreement with the data [34]. For other ground state magnetic moments the contribution from meson-exchange currents is of the order of 0.3μ or smaller with AV18 plus IL7, and with these corrections included, the calculated magnetic moments are generally closer to the data.

Another surprisingly large discrepancy between the calculated and experimental magnetic moment occurs for ${}^{13}\text{N}$. JISP16 gives a negative magnetic moment of about $-0.3(1)\mu$, in sharp contrast to the positive experimental value of $+0.322\mu$. Note that the calculation for the mirror nucleus, ${}^{13}\text{C}$, is in good agreement with the data. It would be interesting to see what one gets with other realistic interactions, and what the meson-exchange contributions are for this case.

Acknowledgements

I would like to thank J. P. Vary, A. M. Shirokov, M. A. Caprio for valuable discussions. This work was supported in part by the National Science Foundation under Grant No. PHY-0904782 and the Department of Energy under Grant Nos. DE-

FG02-87ER40371 and DESC0008485 (SciDAC-3/NUCLEI). A portion of the computational resources were provided by the National Energy Research Scientific Computing Center (NERSC), which is supported by the DOE Office of Science under Contract No. DE-AC02-05CH11231, and by an INCITE award, "Nuclear Structure and Nuclear Reactions", from the DOE Office of Advanced Scientific Computing Research. This research also used resources of the Oak Ridge Leadership Computing Facility at ORNL, which is supported by the DOE Office of Science under Contract DE-AC05-00OR22725, and of the Argonne Leadership Computing Facility at ANL, which is supported by the DOE Office of Science under Contract DE-AC02-06CH11357.

References

- [1] B. R. Barrett, P. Navrátil and J. P. Vary, *Progr. Part. Nucl. Phys.* **69**, 131 (2013) and references therein.
- [2] A. M. Shirokov, J. P. Vary, A. I. Mazur and T. A. Weber, *Phys. Lett. B* **644**, 33 (2007).
- [3] M. Moshinsky, Yu. F. Smirnov, *The harmonic oscillator in modern physics*. Harwood Academic Publishers, 1996.
- [4] P. Maris, J. P. Vary and A. M. Shirokov, *Phys. Rev. C* **79**, 014308 (2009).
- [5] P. Sternberg, E. G. Ng, C. Yang, P. Maris, J. P. Vary, M. Sosonkina and H. V. Le, *Accelerating configuration interaction calculations for nuclear structure*, in *Proc. 2008 ACM/IEEE conf. on Supercomputing*. IEEE Press, Piscataway, NJ, 2008, p. 15:1.
- [6] P. Maris, M. Sosonkina, J. P. Vary, E. G. Ng and C. Yang, *Proc. Comput. Sci.* **1**, 97 (2010).
- [7] H. M. Aktulga, C. Yang, E. G. Ng, P. Maris and J. P. Vary, *Topology-aware mappings for large-scale eigenvalue problems*, in *Euro-Par*, eds. C. Kaklamanis, T. S. Papatheodorou and P. G. Spirakis. *Lecture Notes Comput. Sci.* **7484**, 830 (2012).
- [8] H. M. Aktulga, C. Yang, E. G. Ng, P. Maris and J. P. Vary, *Improving the scalability of symmetric iterative Eigensolver for multi-core platforms*, *Concurrency Computat.: Pract. Exper.* (2013), DOI: 10.1002/cpe.3129.
- [9] C. Yang, H. M. Aktulga, P. Maris, E. Ng and J. Vary, *see these Proceedings*, p. 272, <http://www.ntse-2013.khb.ru/Proc/Yang.pdf>.
- [10] H. Potter, D. Oryspayev, P. Maris, M. Sosonkina, J. Vary, S. Binder A. Calci, J. Langhammer, R. Roth, Ü. Çatalyürek and E. Saule, *see these Proceedings*, p. 263, <http://www.ntse-2013.khb.ru/Proc/Sosonkina.pdf>.
- [11] S. A. Coon, M. I. Avetian, M. K. G. Kruse, U. van Kolck, P. Maris and J. P. Vary, *Phys. Rev. C* **86**, 054002 (2012).
- [12] R. J. Furnstahl, G. Hagen and T. Papenbrock, *Phys. Rev. C* **86**, 031301 (2012).
- [13] S. N. More, A. Ekstrom, R. J. Furnstahl, G. Hagen and T. Papenbrock, *Phys. Rev. C* **87**, 044326 (2013).
- [14] S. A. Coon and M. K. G. Kruse, *see these Proceedings*, p. 314, <http://www.ntse-2013.khb.ru/Proc/Coon.pdf>.
- [15] P. Maris and J. P. Vary, *Int. J. Mod. Phys. E* **22**, 1330016 (2013).

-
- [16] N. Barnea, W. Leidemann and G. Orlandini, *Phys. Rev. C* **74**, 034003 (2006).
- [17] S. Vaintraub, N. Barnea and D. Gazit, *Phys. Rev. C* **79**, 065501 (2009).
- [18] T. Abe, P. Maris, T. Otsuka, N. Shimizu, Y. Utsuno and J. P. Vary, *Phys. Rev. C* **86**, 054301 (2012).
- [19] T. Abe, P. Maris, T. Otsuka, N. Shimizu, Y. Tsunoda, Y. Utsuno and J. P. Vary, *see these Proceedings*, p. 294, <http://www.ntse-2013.khb.ru/Proc/Abe.pdf>.
- [20] T. Dytrych, K. D. Sviratcheva, C. Bahri, J. P. Draayer and J. P. Vary, *Phys. Rev. C* **76**, 014315 (2007).
- [21] T. Dytrych, J. P. Draayer, K. D. Launey, P. Maris, J. P. Vary and D. Langr, *see these Proceedings*, p. 62, <http://www.ntse-2013.khb.ru/Proc/Dytrych.pdf>.
- [22] M. A. Caprio, P. Maris and J. P. Vary, *Phys. Rev. C* **86**, 034312 (2012); *see also these Proceedings*, p. 325, <http://www.ntse-2013.khb.ru/Proc/Caprio.pdf>.
- [23] G. Negoita, *PhD thesis*. Iowa State University, 2010, ProQuest 3418277, <http://gradworks.umi.com/3418277.pdf>.
- [24] A. M. Shirokov, V. A. Kulikov, P. Maris, A. I. Mazur, E. A. Mazur and J. P. Vary, *EPJ Web Conf.* **3**, 05015 (2010).
- [25] A. M. Shirokov, A. I. Mazur, J. P. Vary and E. A. Mazur, *Phys. Rev. C* **79**, 014610 (2009).
- [26] C. Cockrell, J. P. Vary and P. Maris, *Phys. Rev. C* **86**, 034325 (2012).
- [27] S. Baroni, P. Navrátil and S. Quaglioni, *Phys. Rev. C* **87**, 034326 (2013).
- [28] G. Papadimitriou, J. Rotureau, N. Michel, M. Ploszajczak and B. R. Barrett, [arXiv:1301.7140 \[nucl-th\]](https://arxiv.org/abs/1301.7140) (2013).
- [29] J. Rotureau, *see these Proceedings*, p. 236, <http://www.ntse-2013.khb.ru/Proc/Rotureau.pdf>.
- [30] M. A. Caprio, P. Maris and J. P. Vary, *Phys. Lett. B* **719**, 179 (2013).
- [31] P. Maris, *J. Phys. Conf. Ser.* **402**, 012031 (2012).
- [32] G. Audi, O. Bersillon, J. Blachot and A. H. Wapstra, *Nucl. Phys. A* **624**, 1 (1997).
- [33] L. E. Marcucci, M. Pervin, S. C. Pieper, R. Schiavilla and R. B. Wiringa, *Phys. Rev. C* **78**, 065501 (2008).
- [34] S. Pastore, S. C. Pieper, R. Schiavilla and R. B. Wiringa, *Phys. Rev. C* **87**, 035503 (2013).